

Application of relativistic laser plasmas for the study of nuclear reactions

F Ewald^{1,4}, H Schwoerer¹, S Dusterer¹, R Sauerbrey¹, J Magill², J Galy²,
R Schenkel², S Karsch³, D Habs³ and K Witte³

¹ Institut für Optik und Quantenelektronik, Friedrich-Schiller Universität, Max-Wien-Platz 1,
07743 Jena, Germany

² European Commission, Institute for Transuranium Elements, Postfach 2340, 76125 Karlsruhe,
Germany

³ Max-Planck-Institut für Quantenoptik, 85748 Garching, Germany

E-mail: ewald@ioq.uni-jena.de

Received 11 July 2003

Published 10 November 2003

Online at stacks.iop.org/PPCF/45/A83

Abstract

Tabletop Ti:sapphire lasers, such as the Jena multi-Terawatt laser, can nowadays reach focused intensities of up to $10^{20} \text{ W cm}^{-2}$. The interaction of this intense light field with a solid target—in our case tantalum—leads to the production of energetic bremsstrahlung x-rays. These are used to induce (γ, n)- and (γ, f)-reactions in ^{181}Ta , ^{129}I , ^{232}Th , ^{238}U and ^9Be . The results are discussed in the context of laser plasma diagnostics and photo transmutation studies on radioactive material.

We also report on fusion experiments in low- Z targets where the fusion neutrons are utilized to characterize ion acceleration processes.

1. Introduction

Today's most intense light fields that can be produced within a laboratory are generated with near infrared ultrashort-pulse lasers. If the light beam of these lasers is tightly focused within space and compressed in time, the intensity in this focus reaches up to $I = 10^{21} \text{ W cm}^{-2}$, corresponding to an electric field of $E = 10^{12} \text{ V cm}^{-1}$. Thus, the maximum electric field in the laser focus is two orders of magnitude higher than the electric field between the electron and proton in the hydrogen atom which is $E = 5 \times 10^9 \text{ V cm}^{-1}$. Since in the K-shell the electric field scales with Z^3 , $10^{12} \text{ V cm}^{-1}$ is just the field that binds a K-shell electron in the carbon atom. Consequently, matter which particularly consists of light elements is turned into a fully ionized plasma, when placed into the intense light field.

Since the average binding energy per nucleon in the nucleus is of the order of 8 MeV, $10^{12} \text{ V cm}^{-1}$ is by far not sufficient to produce a measurable effect on the nucleus itself. If a nucleon is supposed to be separated from the nucleus only under the influence of an electric

⁴ Author to whom any correspondence should be addressed.

field, about 10^7 V would be required within a length of the size of the nucleus of 10^{-12} cm. That is, 10^{19} V cm $^{-1}$, which is seven orders of magnitude higher than the electric field generated inside the laser focus. Consequently, it is presently not possible to induce nuclear reactions directly through high intensity infrared laser light.

However, at intensities above $I_L > 3 \times 10^{18}$ W cm $^{-2}$ the quiver energy of an electron in the focus exceeds its rest mass energy. In this relativistic regime the magnetic part of the Lorentzian force ($e\vec{v} \times \vec{B}$) becomes comparable to the electric force ($e\vec{E}$), which results in an acceleration of electrons not only in the direction of the electric field vector but also in the direction of light propagation. In a light field with a wavelength of $\lambda = 800$ nm and an electric field of $E_L = 10^{12}$ V cm $^{-1}$ the electron energy is about 10 MeV. These fast electrons efficiently generate high energy bremsstrahlung if they are stopped in a solid target with high atomic number Z .

Both, the hard bremsstrahlung photons and the relativistic electrons, may induce nuclear reactions. In this report we demonstrate the transmutation of several isotopes through neutron emission from nuclei ((γ, n) -reactions) and through fission reactions ((γ, f)), both induced by bremsstrahlung from laser generated plasmas.

In the plasma, not only electrons, but also ions can be accelerated to several hundreds of MeV [5] and are potential projectiles for inducing nuclear reactions [24, 17]. In the last section of this manuscript we will show that efficient fusion of deuterium is accomplished in laser plasmas generated on heavy water droplets. The fusion reaction of deuterium ions is also used as a monitor for two different ion acceleration mechanisms that are discussed in [13].

The field of laser induced nuclear reactions is still very young because laser intensities exceeding 10^{19} W cm $^{-2}$ have become available only in the last few years. The high energy emissions from laser plasmas can be characterized by nuclear activation measurements. In turn, laser induced nuclear reactions begin to be valuable for the investigation of transmutation scenarios or isotope production as compact and versatile methods.

2. Suprathermal electrons and bremsstrahlung

During the interaction of an intense laser pulse with solid matter, a plasma is formed by weak pre-pulses and spontaneous amplified emission, which always precede the main laser pulse. Even though electrons in this pre-plasma have thermal energies, the interaction between the high intensity part of the pulse with the preformed plasma causes heating of electrons to suprathermal energies. The relativistic electrons, generated by the electromagnetic field and by the ponderomotive force associated with the spatial structure of the laser pulse [21], heat the plasma by collisions with the solid target. Depending on the pre-plasma conditions and the interaction geometry, these absorption mechanisms are referred to as vacuum heating [4] or $(j \times B)$ -heating [15]. Furthermore, the laser light can resonantly couple to plasma waves at the critical plasma density (resonance absorption [16]), which are dissipated and heat the plasma. In underdense regions of the plasma, a propagating intense light pulse can generate a density wave behind it with a velocity close to the speed of light, the so-called laser wake field [31]. This again accelerates electrons to relativistic energies. In relativistic self-focused filaments or channels electrons are effectively accelerated by direct laser acceleration [9, 25]. These electron acceleration mechanisms are multi-faceted and not clearly separable within an experiment, since they sensitively depend on the laser intensity, temporal pulse shape, target material, etc. All acceleration mechanisms can be responsible for heating of electrons to energies of several MeV up to 200 MeV [22]. The energy of these suprathermal electrons is typically described by a single or double exponential slope [9, 2]. However, for the applications discussed in this

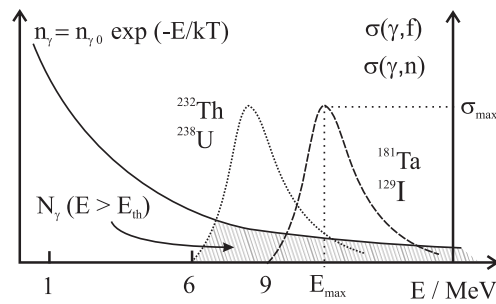


Figure 1. Schematic illustration of the nuclear activation technique for measuring the photon temperature of laser generated bremsstrahlung. The solid line and the dotted and dashed lines represent the bremsstrahlung spectrum and cross sections for nuclear reactions with different threshold energies, respectively. See text for further explanation.

paper, only the high energy tail of the distribution is important. We will therefore adopt the Boltzmann distribution $n = n_0 e^{-E/kT}$ which is commonly used as a good approximation to the real electron spectrum (with E being the electron energy, $kT =: T_e$ the electron ‘temperature’ and n_0 a normalization factor). Electron temperatures of up to $T_e = 9$ MeV have been measured in laser–solid interactions [20]. The number of accelerated electrons is determined by the conversion efficiency from laser energy into energy of relativistic electrons of up to 40% [14, 32, 11].

With conversion efficiencies ($E_\gamma/E_{\text{laser}}$) of a few per cent [11], high energy bremsstrahlung radiation is generated in solid-density high- Z targets. The spectral distribution of these photons is again Boltzmann shaped [23] with typical temperatures of 1–3 MeV and maximum energies of tens of MeV at laser intensities of $10^{20} \text{ W cm}^{-2}$. An appropriate scaling of the electron temperature T_e with intensity is $T_e \sim (I\lambda^2)^{1/2}$, which is valid particularly at laser intensities above $10^{18} \text{ W cm}^{-2}$ [33, 10]. While the hot electron temperature T_e is thus determined by the intensity of the focused laser pulse, the number of accelerated electrons pre-dominantly depends on the pulse energy.

Measuring the spectral distribution of these high energy photons is a challenging task. Spectra were measured with thermoluminescence dosimeter (TLD) based spectrometers [2], which provide reliable data up to γ -energies of about 3 MeV. Beyond this limit alternative methods have to be used. One possible way of measuring the bremsstrahlung and electron temperatures is the activation of nuclei by γ -induced reactions. This method has already been demonstrated by a number of groups [26, 6, 18, 28, 20, 30, 27]. A γ -photon that is incident on a nucleus can excite the giant resonances of nuclei and thereby for example induce fission reactions (γ, f) or the emission of a neutron (γ, n). Such γ -induced nuclear reactions have discrete energy thresholds in the MeV range. This covers the energy range at which the bremsstrahlung is intended to be measured. As illustrated in figure 1, the number N_γ of bremsstrahlung photons with energies above the reaction threshold (hatched) can be determined from the number of induced reactions and the cross section (dotted, dashed) weighted with the exponential γ -distribution.

3. Photo induced nuclear reactions

The experimental set-up which has been used in most of the experiments presented herein, as well as the Jena multi-Terawatt laser system, are described in greater detail in [27, 8]. The plasma is generated by a laser pulse that concentrates up to 400 mJ in 70 fs focusable to a

spot size of $5 \mu\text{m}^2$. This leads to an intensity of $10^{20} \text{ W cm}^{-2}$. In this intense light field the surface of the target material, which is chosen to be tantalum in this experiment, is turned into a hot plasma. As described in the previous section, bremsstrahlung is generated in this target by suprathreshold electrons. The bremsstrahlung radiation can directly induce nuclear reactions in tantalum or it can be used to induce reactions in other samples which are placed inside the γ -radiation field directly behind the tantalum bremsstrahlung converter. The latter has been the case for the samples ^{129}I , ^{232}Th and ^{238}U . The remaining nuclei of the (γ, n) - or (γ, f) -reactions are usually unstable and can therefore be detected by their characteristic γ -emissions and half-lives. After irradiation with about 10 000 laser shots, the samples were taken out of the target chamber and measured with a high-purity germanium- γ spectrometer. Since the energy dependent efficiency of the detector is known, absolute numbers of induced reactions are obtained from the activity of the samples.

The first nuclear reaction which was demonstrated using a tabletop Ti : sapphire laser was the (γ, n) -reaction of ^9Be [28, 7]. The threshold energy of 1.67 MeV is the lowest threshold of γ -induced reactions. This reaction is therefore within reach already at laser intensities of a few times $10^{18} \text{ W cm}^{-2}$.

At even higher intensities of up to $10^{20} \text{ W cm}^{-2}$ nuclear reactions with higher energy thresholds are feasible, such as (γ, n) - and (γ, f) -reactions in nuclei with high mass numbers. We will now concentrate on (γ, n) -reactions, in which a photon impinging on a nucleus causes the emission of a neutron, leaving a nucleus with a mass number which is reduced by one.

Taking as an example the (γ, n) -reaction in ^{181}Ta , we will now illustrate the nuclear activation technique, which leads to an absolute number of photons with energies above the reaction threshold. ^{181}Ta has a reaction threshold of 7.56 MeV for the $^{181}\text{Ta}(\gamma, n)^{180}\text{Ta}$ -reaction. With a probability of 86%, the resulting isotope ^{180}Ta decays into ^{180}Hf via electron capture and with 14% by β^- -decay to ^{180}W . The half-life of ^{180}Ta is 8.15 h. Due to the electron capture reaction, intense characteristic Hf x-ray lines occur in the γ -spectrum, which were used to detect the decay from ^{180}Ta to ^{180}Hf (figure 2) after irradiation with laser produced bremsstrahlung. A total number of 160 reactions was induced with one laser shot, concentrating 250 mJ of energy to an intensity of $4 \times 10^{19} \text{ W cm}^{-2}$. Assuming an exponential bremsstrahlung distribution with a temperature of $kT = 1.2 \text{ MeV}$, which was determined from measurements with TLD spectrometers, it is found that about 10^5 photons with energies above 7.6 MeV were incident on the tantalum target.

Conversely, an experiment is conceivable in which the cross section of a photo induced reaction is determined from the known photon distribution and from the number of induced reactions. Such a reaction is the transmutation of the radioactive isotope ^{129}I by a (γ, n) -reaction. Thereby ^{129}I , which has a half-life of 10^5 years, is converted into ^{128}I that decays with a half-life of only 25 min into the stable and inert gas ^{128}Xe . We have successfully induced this reaction with our tabletop laser system and we were able to estimate a value of the cross section σ_{max} at the giant resonance energy E_{max} . The γ -line at 443 keV from the decaying ^{128}I (figure 3) has been used to determine the number of induced γ -reactions. The (γ, n) -reaction cross section of ^{129}I has never been measured before. Only the threshold energy is known from calculations to be 8.8 MeV [34]. Typically the giant resonance cross sections have a Lorentzian-like shape and it can be assumed that both the giant resonance energy E_{max} (see figure 1) and the full width at half maximum have values very similar to those of ^{127}I ($E_{\text{max}} = 15 \text{ MeV}$, FWHM = 5 MeV). Therewith a cross section value at the giant resonance energy of $\sigma_{\text{max}} = (220_{-100}^{+230}) \text{ mbarn}$ has been estimated from the measured number of reactions. To our knowledge, this is the first determination of the (γ, n) -cross section of ^{129}I .

This cross section value is particularly interesting because ^{129}I is one of the most important and hazardous isotopes contained in spent fuel from nuclear power plants. In the context of

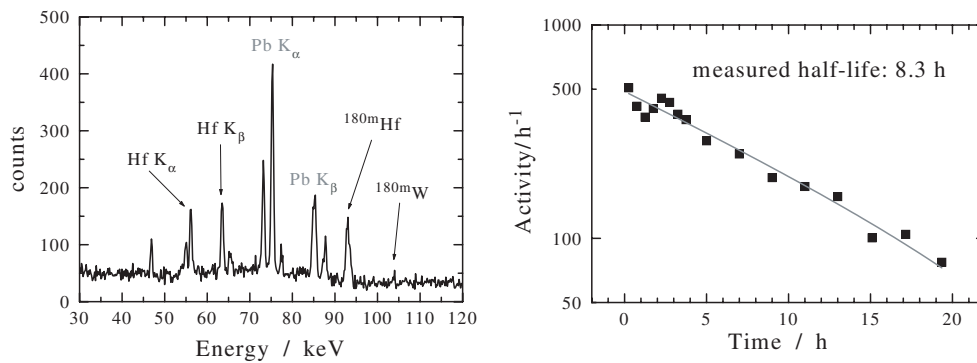


Figure 2. Left-hand side: spectrum of the activated tantalum, measured with a HPGe-detector. The Hf- K_{α} -lines were taken for evaluation of the activity. In addition to the x-ray lines, two γ -lines from the decay to ^{180}Hf and ^{180}W occur at 93 keV and 103 keV, respectively. Right-hand side: activity of the Hf K_{α} -line as it depends on time. The measured half-life of the ^{180}Ta -decay is in very good agreement with the tabulated value of 8.15 h.

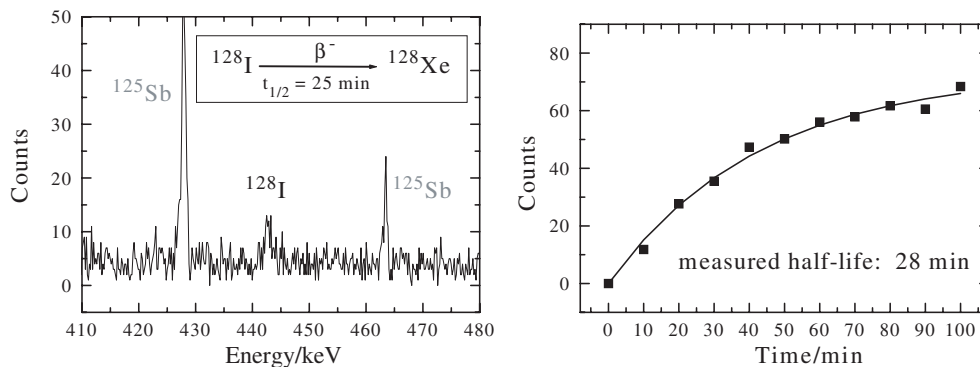


Figure 3. Detection of the photo induced transmutation of ^{129}I . Left-hand side: spectrum of the irradiated iodine sample. The area under the 443 keV-line originating from the β^{-} -decay to ^{128}Xe was measured as it depends on time (right graph). Impurities in the sample cause the ^{125}Sb -lines. Right graph: the data (■) was fitted with a function of the form $1 - \exp(-\ln 2 t / \tau)$ (—), resulting in a half-life of (28 ± 5) min. Therewith it could be verified that the detected γ -line originates from the decaying ^{128}I (tabulated value: $t_{1/2} = 25$ min).

partitioning and transmutation programmes [1] particular attention is paid to the study of transmutation mechanisms, which also includes the investigation of yet unknown reaction parameters and different kinds and combinations of particle and photon induced reactions. Since the tabletop laser combines its compactness with a brilliant source of γ -rays and particles such as relativistic electrons, energetic protons, neutrons and ions, it lends itself to these kinds of studies.

In contrast to nuclei with moderate mass numbers such as ^{129}I or ^{181}Ta , heavy nuclei such as ^{238}U or ^{232}Th exhibit a high cross section for photofission. The threshold energy for the (γ, f) -reactions of these two isotopes is only 6 MeV. Therefore ^{238}U has been the first nucleus for which laser induced fission has been proposed [3] and experimentally verified [18, 6, 20, 27]. Only recently, ^{232}Th has been fissioned for the first time by laser produced bremsstrahlung [27]. From the isotopes accruing during the fission reaction the number of induced reactions has been determined to be about 100 per laser shot [8].

4. Laser induced fusion and ion acceleration mechanisms

Besides photons and electrons, also plasma ions and protons can be accelerated up to MeV energies [12, 19]. Under specific conditions the acceleration gradient can be 200 GeV m^{-1} which is considerably larger than in conventional linear accelerators [31, 22]. However, the physics behind the acceleration mechanisms of ions is not yet fully understood. Currently, two mechanisms of ion acceleration are under discussion: first, a strong electrostatic field is formed due to the ponderomotive charge separation at the front surface of the target and causes an acceleration of the ions into the target [5]. The second mechanism describes the acceleration of ions from the rear surface of the target due to laser heated electrons that traverse the target and generate a space charge at the rear target surface when leaving the material. Ions are pulled out of the target and are accelerated in this electrostatic field. In the literature this mechanism is referred to as target-normal sheath acceleration (TNSA) [11, 29, 12].

To observe both acceleration mechanisms in one single experiment, we used the fusion reaction of deuterium ions $d(d,n)^3\text{He}$ [13]. Heavy water (D_2O) droplets were irradiated with a laser pulse of $3 \times 10^{19} \text{ W cm}^{-3}$. Under the exposure to this intense light field, deuterium is ionized. The ions are then accelerated and undergo fusion reactions. The energy of the resulting fusion neutrons which is 2.45 MeV is superimposed by the centre-of-mass energy of the reacting deuterons. This kinematic shift of the neutron energy gives rise to a broader energy distribution which provides information on the incident deuteron energy. Figure 4 illustrates how neutrons from the droplet front and rear surface are detected separately by time of flight (TOF) spectroscopy: at the front side of the droplet, deuterium ions are accelerated by the ponderomotive charge separation and undergo fusion reactions. The stopping range of the deuteron ions in the water droplet is much smaller than the droplet thickness, such that the ions cannot traverse the target. Thus, the detected fusion neutrons only monitor the ion acceleration at the front side of the droplet. The TOF spectrum corresponding to this neutron population is shown in figure 5(a). From the energy distribution of the neutrons the

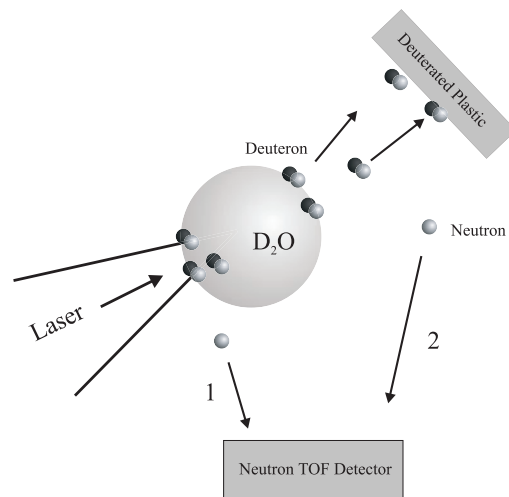


Figure 4. Sketch of the experimental discrimination of front and rear side ion acceleration in targets being thick compared to the ion path-length. The neutrons marked with 1 are generated by fusion reactions at the front side of the target. The neutrons numbered with 2 are due to delayed fusion in an additional deuterated plastic target ('catcher') which is placed a few centimetres behind the droplet.

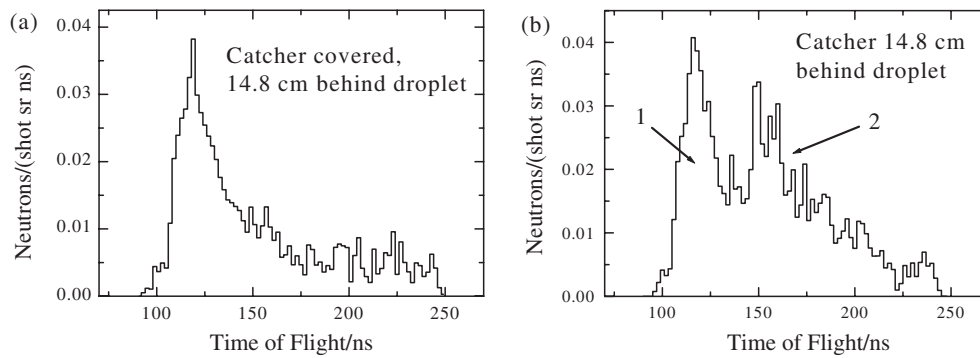


Figure 5. Neutron TOF spectra (a) without and (b) with the deuterated piece of plastic. The two peaks in (b) which are numbered 1 and 2 are related to the neutron populations shown in figure 4. The time lag between the two neutron peaks is mainly given by the TOF of deuterons from the rear side of the droplet to the catcher. From this time an ion temperature of 100 keV for the rear side ions is derived.

temperature of the ions that are accelerated at the target front side is determined to be about 350 keV. Deuterons accelerated at the rear side of the droplet induce delayed fusion reactions in a deuterated plastic target ('catcher'), which is placed behind the droplet. The neutrons arising from these fusion reactions are detected at later flight times and produce the second neutron peak in the TOF spectrum shown in figure 5(b). Since the water droplet is only transparent for energetic electrons and not for ions from the front side, rear side ions can only be accelerated by the TNSA mechanism. Thus, for the first time, both ion acceleration mechanisms could be separated in the same experiment, demonstrating that they both take place simultaneously and are not mutually exclusive.

Besides this result, the D_2O -droplet target is a source of MeV neutrons. In the above experiment we were able to generate some 10^4 neutrons per laser shot. The special features of this neutron source are its very small source size and short pulse duration. A further benefit of laser neutron sources is the possibility to switch the neutrons on and off at any time since there is no nuclear chain reaction involved.

5. Conclusion

It has been shown in this paper that relativistic laser plasmas, which are generated with high intensity tabletop lasers like the Jena multi-Terawatt system, are sources of MeV γ -radiation and particles such as relativistic electrons and high energy ions. These particles can be used to induce nuclear disintegration reactions such as the generation of photo neutrons or photo fission. Photon- and particle-induced reactions are very interesting in the context of transmutation of nuclear waste. However, the laser should presently not be understood as a potential device for the disposal of sizeable amounts of radioactive material. But the laser plasma is an interesting particle source for transmutation studies, i.e. for the investigation of possible transmutation pathways. There are two striking attributes of the tabletop laser that qualify it for this kind of research: besides its compactness and high repetition rate, the laser plasma combines a variety of high energy particles in one single source, which is not achievable with any conventional particle accelerator.

A number of applications of laser induced nuclear reactions is conceivable, such as the above-mentioned investigation of reaction pathways in transmutation scenarios as well as the

production of short-lived radioactive isotopes that are used in medical applications, such as positron emission tomography.

Acknowledgments

This work has been funded by the German Science Foundation (DFG) and by the German Ministry for Education and Research (BMBF).

Note added in proof

Experimental details on laser transmutation of ^{129}I were published recently [35, 36].

References

- [1] Baetsle L H, Magill J and Embid-Segura M 2003 Implications of partitioning and transmutation in radioactive waste management *IAEA-TECDOC* submitted
- [2] Behrens R, Schwoerer H, Düsterer S, Ambrosi P, Pretzler G, Karsch S and Sauerbrey R 2003 A TLD-based few-channel spectrometer for simultaneous detection of electrons and photons from relativistic laser-produced plasmas *Rev. Sci. Instrum.* **74** 961–8
- [3] Boyer K, Luk T S and Rhodes C K 1988 Possibility of optically induced nuclear fission *Phys. Rev. Lett.* **60** 557
- [4] Brunel F 1987 Not-so-resonant, resonant absorption *Phys. Rev. Lett.* **59** 52
- [5] Clark E L, Krushelnick K, Zepf M, Beg F N, Tatarakis M, Machacek A, Santala M I K, Watts I, Norreys P and Dangor A E 2000 Energetic heavy-ion and proton generation from ultraintense laser–plasma interactions with solids *Phys. Rev. Lett.* **85** 1654
- [6] Cowan T E *et al* 2000 Photonuclear fission from high energy electrons from ultraintensive laser–solid interactions *Phys. Rev. Lett.* **84** 903
- [7] Düsterer S, Schwoerer H, Behrens R, Ziener C, Reich C, Gibbon P and Sauerbrey R 2001 Hard x-rays and nuclear reactions from laser produced plasmas *Contrib. Plasma Phys.* **41** 171–4
- [8] Ewald F, Schwoerer H, Magill J, Galy J, Schenkel R and Sauerbrey R 2003 Laser induced nuclear reactions, ed P C Ferenc Krausz and Georg Korn *Ultrafast Optics IV (Springer Series in Optical Sciences)* (Berlin: Springer) at press
- [9] Gahn C, Tsakiris G D, Pukhov A, Meyer-ter Vehn J, Pretzler G, Thirolf P, Habs D and Witte K J 1999 Multi-MeV electron beam generation by direct laser acceleration in high-density plasma channels *Phys. Rev. Lett.* **83** 4772
- [10] Gibbon P and Förster E 1996 Short-pulse laser–plasma interactions *Plasma Phys. Control. Fusion* **38** 769–93
- [11] Hatchett S P *et al* 2000 Electron, photon, and ion beams from the relativistic interaction of Petawatt laser pulses with solid targets *Phys. Plasmas* **7** 2076
- [12] Hegelich M *et al* 2002 MeV ion jets from short-pulse interaction with thin foils *Phys. Rev. Lett.* **89** 085002
- [13] Karsch S, Düsterer S, Schwoerer H, Ewald F, Habs D, Hegelich M, Pretzler G, Pukhov A, Witte K and Sauerbrey R 2003 High-intensity laser induced ion acceleration from heavy-water droplets *Phys. Rev. Lett.* **91** 015001
- [14] Key M H, Cable M D and *e. a.* Cowan T E 1998 Hot electron production and heating by hot electrons in fast ignitor research *Phys. Plasmas* **5** 1966
- [15] Kruer W L and Estabrook K 1985 $j \times B$ heating by very intense laser light *Phys. Fluids* **28** 430
- [16] Kruer W L 1988 *The Physics of Laser Plasma Interaction* (Redwood-City: Addison-Wesley)
- [17] Ledingham K W D, McKenna P and Singhal R P 2003 Applications for nuclear phenomena generated by ultra-intense lasers *Science* **300** 1107–11
- [18] Ledingham K W D *et al* 2000 Photonuclear physics when a multiterawatt laser pulse interacts with solid targets *Phys. Rev. Lett.* **84** 899
- [19] Mackinnon A J, Sentoku Y, Patel P K, Price D W, Hatchett S, Key M H, Andersen C, Snavely R and Freeman R R 2002 Enhancement of proton acceleration by hot-electron recirculation in thin foils irradiated by ultraintense laser pulses *Phys. Rev. Lett.* **88** 215006
- [20] Malka G *et al* 2002 Relativistic electron generation in interactions of a 30 TW laser pulse with a thin foil target *Phys. Rev. E* **66** 066402
- [21] Malka G and Miquel J L 1996 Experimental confirmation of ponderomotive-force electrons produced by an ultrarelativistic laser pulse on a solid target *Phys. Rev. Lett.* **77** 75

- [22] Malka V *et al* 2002 Electron acceleration by a wakefield forced by intense ultrashort laser pulse *Science* **298** 1598
- [23] McCall G 1982 Calculation of x-ray bremsstrahlung and characteristic line emission produced by a Maxwellian electron distribution *J. Phys. D: Appl. Phys.* **15** 823
- [24] Nemoto K, Maksimchuk A, Banerjee S, Flippo K, Mourou G, Umstadter D and Bychenkov V Y 2001 Laser-triggered ion acceleration and table top isotope production *Appl. Phys. Lett.* **78** 595–7
- [25] Pukhov A and Meyer-ter Vehn J 1999 Relativistic laser–plasma interactions by multi-dimensional particle-in-cell simulations *Phys. Plasmas* **5** 1880
- [26] Santala M I K *et al* 2000 Effect of the plasma density scale length on the direction of fast electrons in relativistic laser–solid interactions *Phys. Rev. Lett.* **84** 1459–62
- [27] Schwoerer H, Ewald F, Sauerbrey R, Galy J, Magill J, Rondinella V, Schenkel R and Butz T 2003 Fission of actinides using a tabletop laser *Europhys. Lett.* **61** 47
- [28] Schwoerer H, Gibbon P, Düsterer S, Behrens R, Ziener C, Reich C and Sauerbrey R 2001 MeV x rays and photoneutrons from femtosecond laser-produced plasmas *Phys. Rev. Lett.* **86** 2317–20
- [29] Snavely R A *et al* 2000 Intense high-energy proton beams from petawatt-laser irradiation of solids *Phys. Rev. Lett.* **85** 2945–348
- [30] Spencer I *et al* 2002 A nearly real-time high temperature laser–plasma diagnostic using photonuclear reactions in tantalum *Rev. Sci. Instrum.* **73** 3801–05
- [31] Tajima T and Dawson J M 1979 Laser electron accelerator *Phys. Rev. Lett.* **43** 267
- [32] Wharton K B, Hatchett S P, Wilks S C, Key M H, Moody J D, Yanovsky V, Offenberger A A, Hammel B A, Perry M D and Joshi C 1998 Experimental measurements of hot electrons generated by ultraintense ($> 10^{19}$ W cm⁻²) laser–plasma interactions on solid-density targets *Phys. Rev. Lett.* **81** 822–5
- [33] Wilks S C, Kruer W L, Tabak M and Langdon A B 1992 Absorption of ultra-intense laser pulses *Phys. Rev. Lett.* **69** 1383
- [34] 2000 Handbook on photonuclear data for applications—cross sections and spectra *IAEA-TECDOC*
- [35] Magill J, Schwoerer H, Ewald F, Galy J, Schenkel R and Sauerbrey R 2003 Laser transmutation of iodine-129 *Appl. Phys. B* **77** 387–90
- [36] Ledingham K W D *et al* 2003 Laser-driven photo-transmutation of ¹²⁹I—a long-lived nuclear waste product *J. Phys. D: Appl. Phys.* **36** L63–6